Analysis 2

Ethan Cline

Center for Frontiers in Nuclear Science

Department of Physics and Astronomy
Stony Brook University

BVR Subcommittee Meeting

This work is supported by the National Science Foundation, grants PHY-2012114 to Stony Brook University. The MUSE experiment is supported by the U.S. Department of Energy, the U.S. National Science Foundation, the Paul Scherrer Institute, and the US-Israel Binational Science Foundation.

January 23, 2023

Stony Brook University

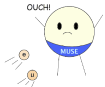

MUSE

Blinding

- Blind at track level using blinding scheme presented by J. C. Bernauer in BVR 52
- Throw out tracks with angular dependence
- A, B are generated from fixed seed and are unique for charge, species, momentum, simulation
- $A = 0.25..1,\ B = 3..10$

$$s = 0.2(A + 0.3\cos(B \times \theta)) \tag{1}$$

$$P = s \times \frac{3 - \theta}{3} \tag{2}$$

- if $P \leq R$, where R is a uniformly distributed random number between 0 and 1, encrypt the track
- Can blind up to 25 % of tracks at any given angle, typically 10 % are blinded
- **All data shown in this talk are blinded**
- Scheme may be implemented in G_{Mn} collaborations at JLab

Example Blinding Curve

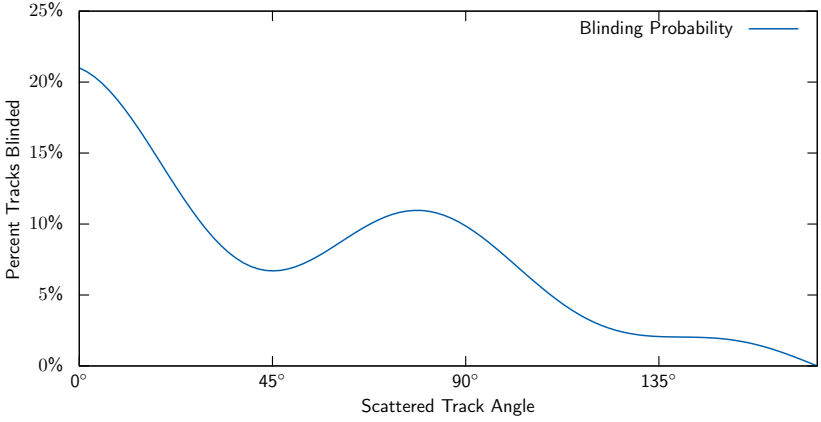

Chance of blinding a track for A = 0.75 and B = 4.2 as a function of STT angle.

Event Selection

- Using TCPV and VETO cuts at event trigger level
- PID in BH - only look at electrons in initial analysis to separate out common issues to all particle types from issues related to reaction identification (scattering vs. decay in flight)
- Track in STT
- Track in GEMs
- Fiducial cuts
- Curves are normalized to the integral in the peak near 0

MUSE Sketch

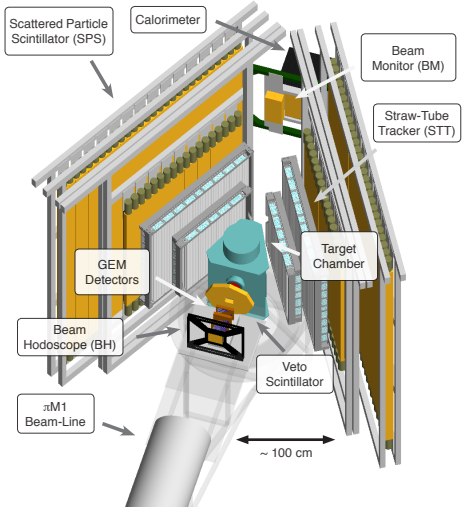
Scattered Particle Scintillator (SPS)
Calorimeter
Beam Monitor (BM)
Straw-Tube Tracker (STT)
GEM Detectors
Target Chamber
Beam Hodoscope (BH)
Veto Scintillator
πM1 Beam-Line
~ 100 cm

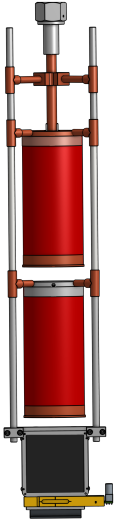

MUSE Solid Target

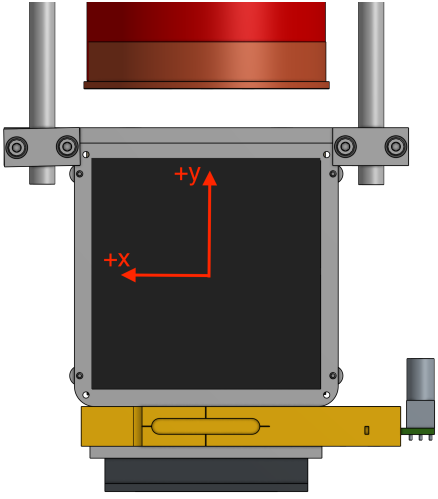

Vertex Reconstruction

- Here we show reconstructed vertices from STT and GEM tracks
- Analysis done for left and right STT, mostly showing left
- $e^- C$ and $e^+ C$ scattering at ± 115 MeV/c
- Cut on distance of closest approach < 5 mm, effective "Track quality" selection

Top-Down view of reconstructed vertices

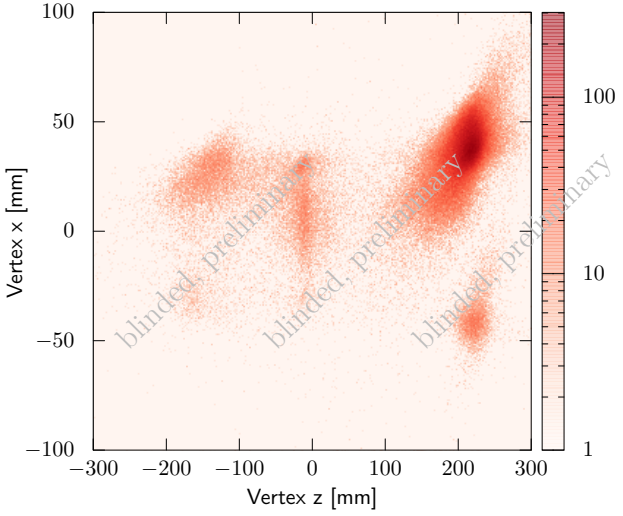

Carbon target x v z vertex reconstruction. Entrance aperture on the left, carbon target in the middle, exit posts on the right. Note excess events on exit post at positive x; this is the post closer to the STT chamber used to construct tracks.

Target distribution at abs(z) < 80 mm

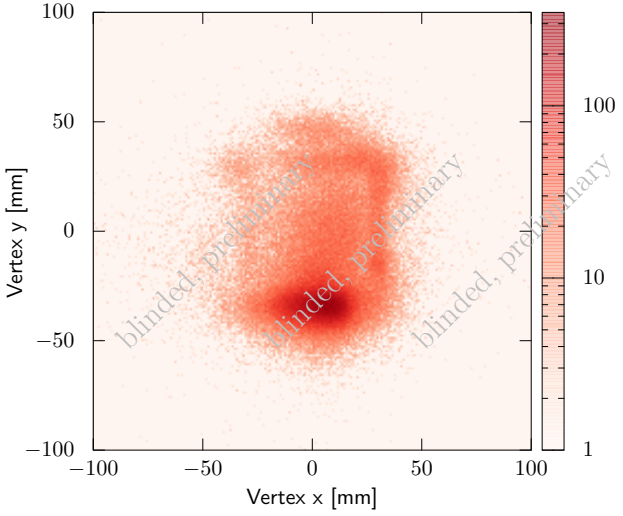

Carbon target y vs. x vertex reconstruction. Apply fiducial cut $y > 0$ to prevent contamination from BFM. Note that $+x$ points toward left STT.

Target distribution at abs(z) < 80 mm

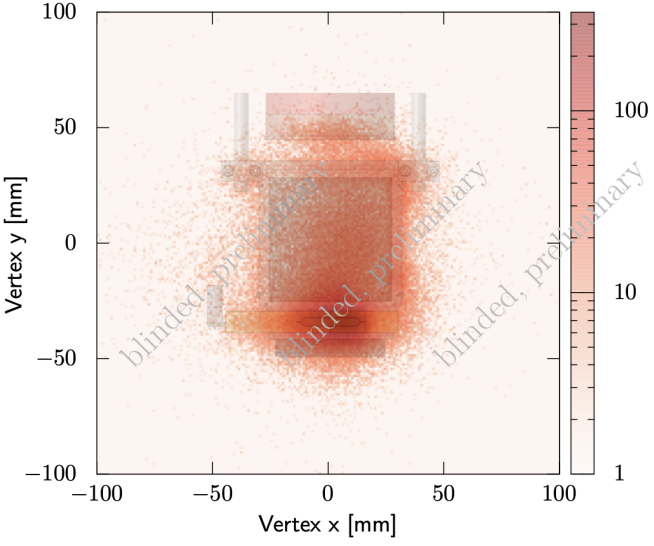

Carbon target y vs. x vertex reconstruction. Apply fiducial cut $y > 0$ to prevent contamination from BFM. Note that $+x$ points toward left STT.

y Vertex

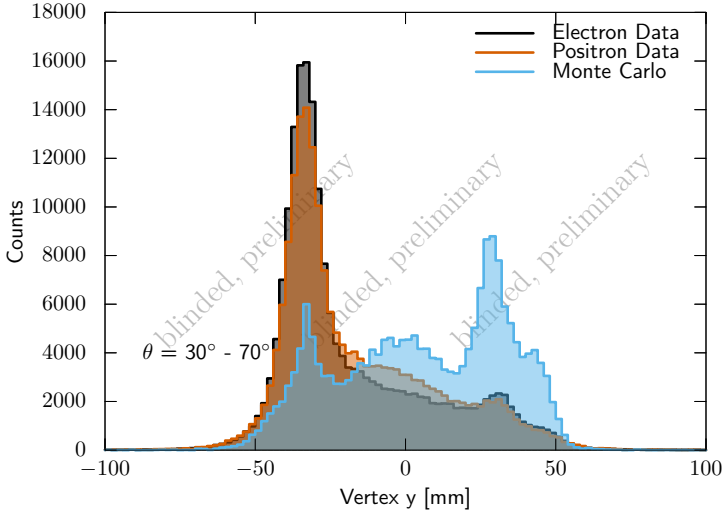

A plot of the reconstructed y vertices from the carbon target. Note the large peak at $y = -40$ mm corresponds to the BFM detector, which is not implemented in the simulation. The peak at $y = 50$ mm corresponds to the bottom end cap of the empty target.

x Vertex

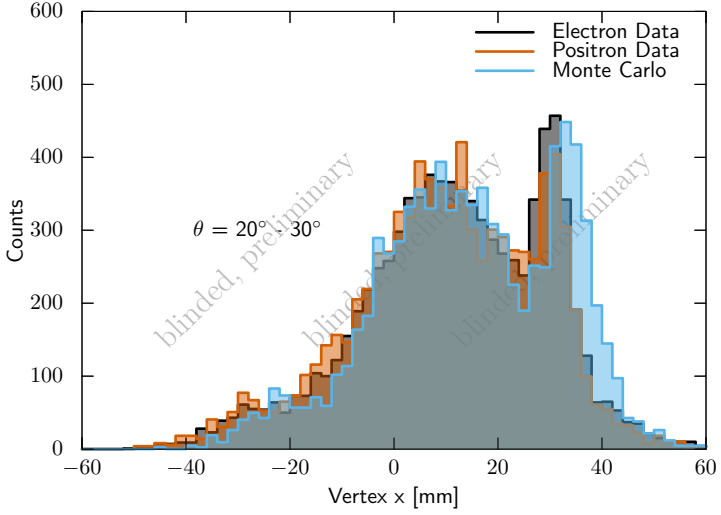

A plot of the reconstructed x vertices from the carbon target. The peak at $x = 35$ mm corresponds to the support post holding the target closest to the STT chamber used in track reconstruction. Note that there is another smaller peak at $x = -25$ mm that corresponds to the other support post.

x Vertex

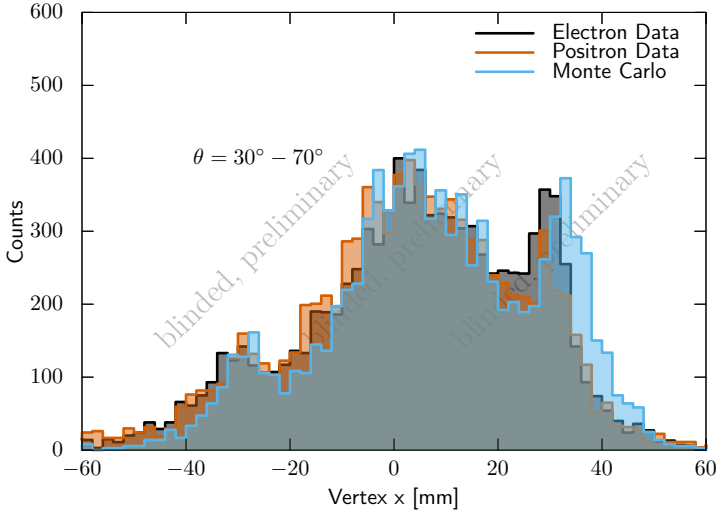

A plot of the reconstructed x vertices from the carbon target. The peak at $x = 35$ mm corresponds to the support post holding the target closest to the STT chamber used in track reconstruction. Note that there is another smaller peak at $x = -25$ mm that corresponds to the other support post.

x Vertex

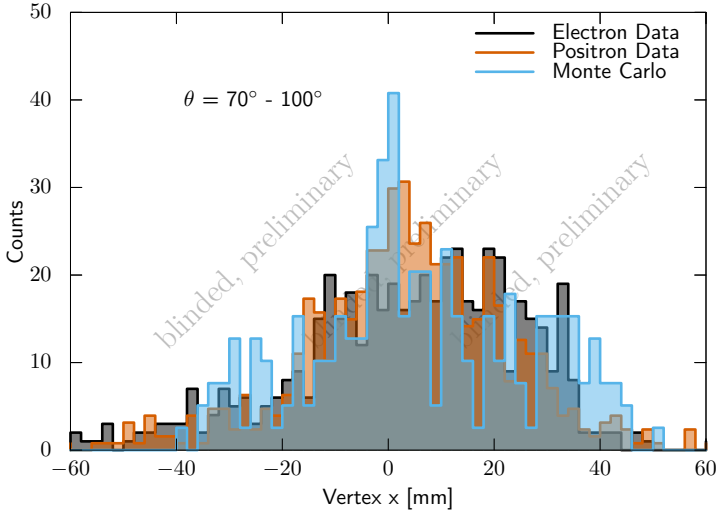

A plot of the reconstructed x vertices from the carbon target. The peak at $x = 35$ mm corresponds to the support post holding the target closest to the STT chamber used in track reconstruction. Note that there is another smaller peak at $x = -25$ mm that corresponds to the other support post.

z Vertex

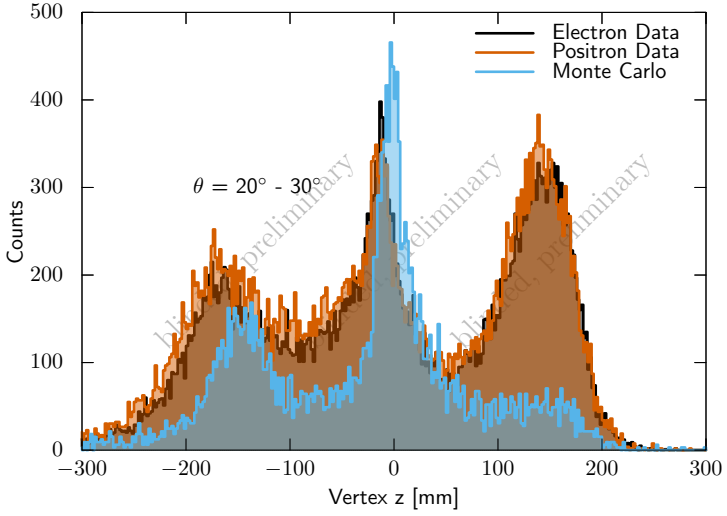

A plot of the reconstructed z vertices from the carbon target. The agreement between electron and position data indicate that the beam properties do not significantly change when cycling the magnets. The offset between the data and simulated target peaks arise from the target survey which is not yet implemented in the simulation.

Z Vertex

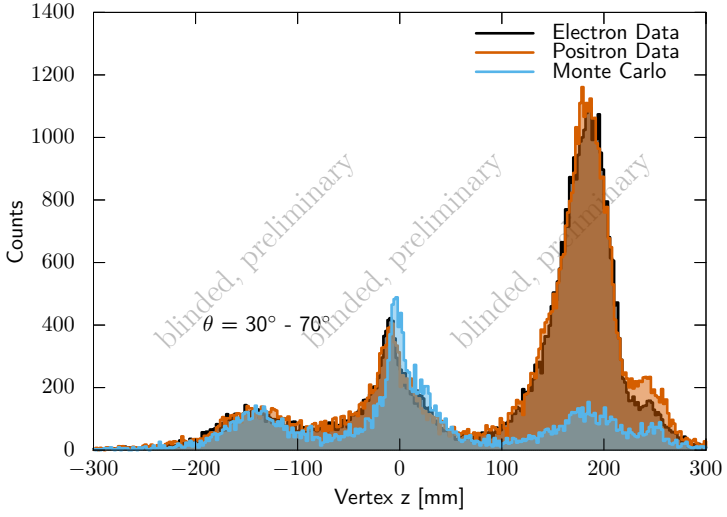

A plot of the reconstructed z vertices from the carbon target. The agreement between electron and position data indicate that the beam properties do not significantly change when cycling the magnets. The offset between the data and simulated target peaks arise from the target survey which is not yet implemented in the simulation.

Z Vertex

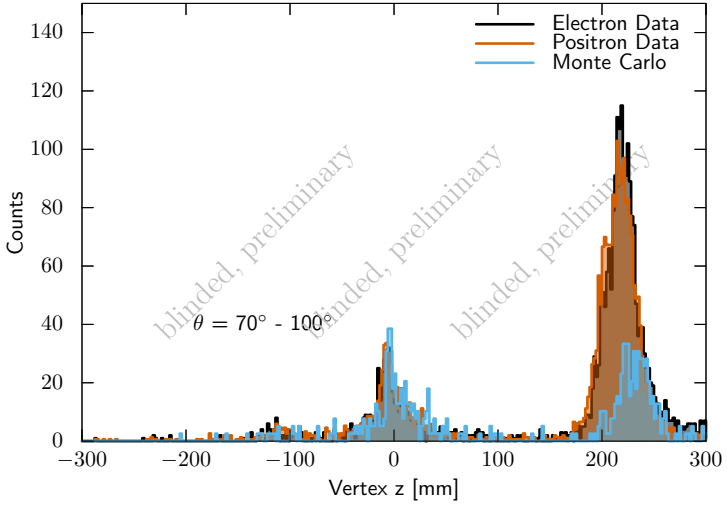

A plot of the reconstructed z vertices from the carbon target. The agreement between electron and position data indicate that the beam properties do not significantly change when cycling the magnets. The offset between the data and simulated target peaks arise from the target survey which is not yet implemented in the simulation.

Z Vertex

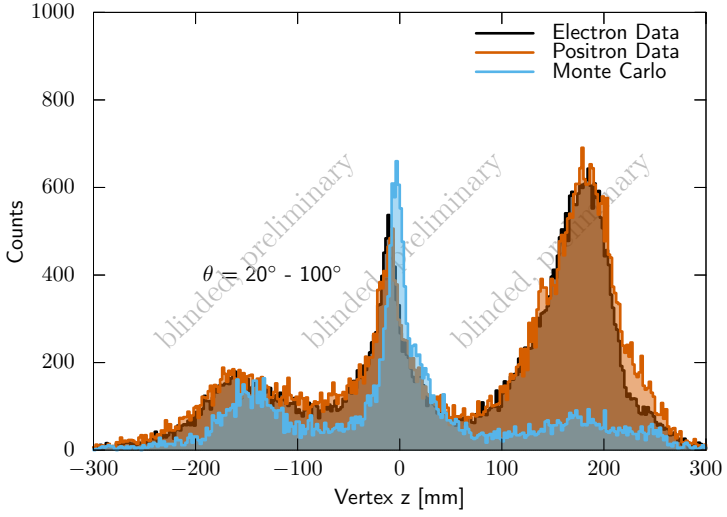

Simulation $\sigma = 12$ mm, data $\sigma = 18$ mm from gaussian fit to peak around target. The different peak position between simulation and data arise from the survey not being included in the simulation.

Z Vertex

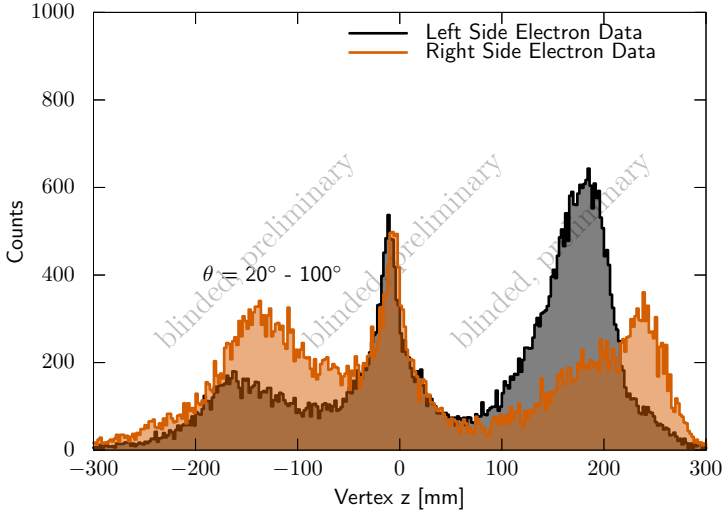

Reconstructed z vertex from the left and right side STT chambers. Note the target width is about the same, but the backgrounds differ. The beam contains $< x'|x >$ correlations, so we expect differences in the relative rate of beam impinging on opposite sides of the chambers.

Scattering Angle

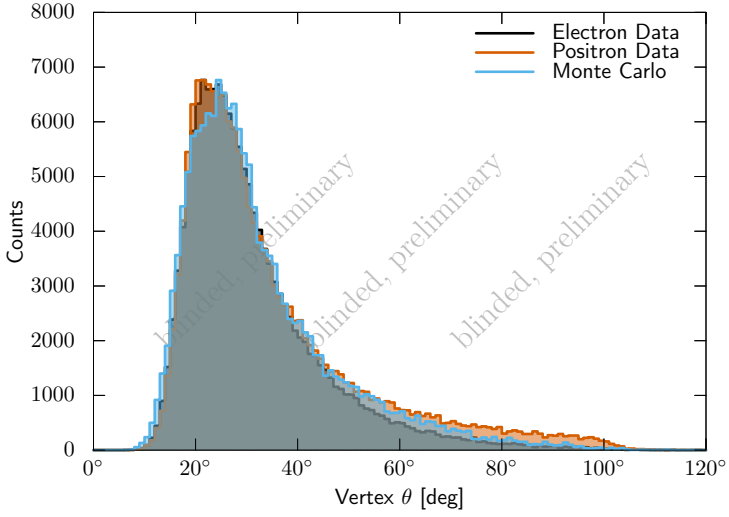

Reconstructed scattering angle from $e^- C$ and $e^+ C$ data and $e^- C$ simulation. Note that radiative corrections are not applied, which can introduce shapes in the scattering angles

Cross Section Extraction

- Measured cross section for $e^{\pm}, \mu^{\pm}, \pi^{\pm}$-^{12}C/H
- Presenting results for $e^{\pm}C$ scattering

$$\frac{d\sigma}{d\Omega}_i = \frac{\mathrm{counts_i}}{N_{beam} n_t \Delta\Omega_i \epsilon_{DAQ} \epsilon_{fiducial} \epsilon_{rad}}, \tag{3}$$

- counts$_i$ given from reconstructed vertices binned in angle
- N_{beam} calculated from BH trigger rates
- n_t carbon areal density
- $\Delta\Omega_i$ estimate of current acceptance. Requires full simulation
- ϵ_{DAQ} (reconstruction efficiency, detector efficiency, live time, etc.) known from analysis
- $\epsilon_{fiducial}$ imposed in analysis
- ϵ_{rad} radiative corrections, taken to be 1 for this analysis

Limitations

- No radiative corrections
  - Private communication with A. Afanasev on radiative corrections for carbon
  - Requires full generator and Monte Carlo implementation
- Survey for 2022 beam time currently underway
  - Have survey data and implementation for application
  - Need to get data into code base
- Full Monte Carlo for acceptance not completed
  - Requires use of computing farm, very time intensive

electron/positron-carbon Scattering

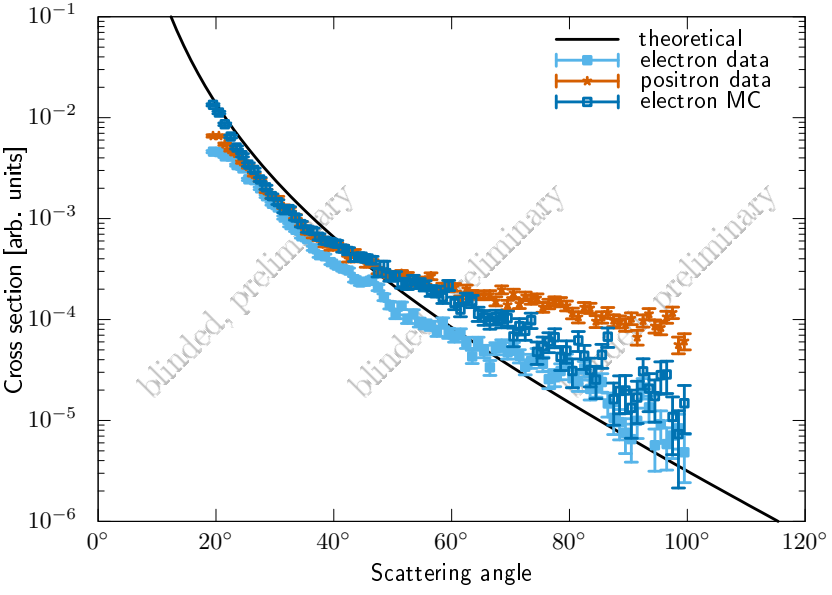

MUSE LH2/Empty Target

- Top cylinder filled with LH_2, bottom empty
- 6 cm diameter
- 13.7 cm tall
- Copper end caps
- 4×25 μm wrapping around cell (not shown)

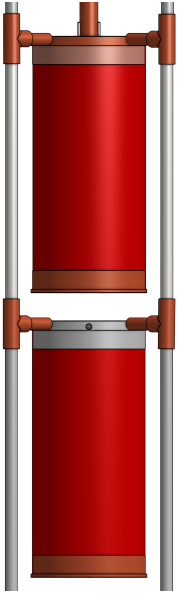

Vertex Reconstruction

- Here we show reconstructed vertices from the STTs and GEMs
- Full and empty cell measurements
- Apply fiducial cuts on target, discussed on next slide
- Cut on distance of closest approach < 10 mm, effective "Track quality" selection
- Data taken at $+160$ MeV/c

Target distribution

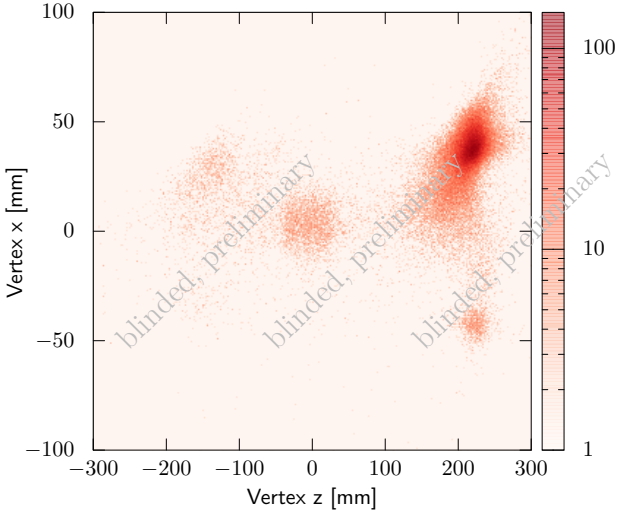

Full target x vs. z vertex reconstruction. Note the entrance aperture on the left and exit posts on the right are visible, as well as the LH_2 target in the center.

Target distribution with cut on abs(z) < 80

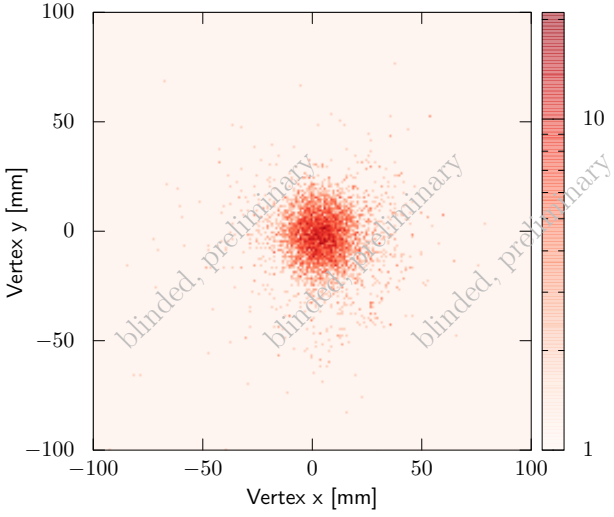

Full target y vs. x vertex reconstruction. In contrast to the carbon target, here we only see the beam spot on the LH_2 target.

LH2 Scattering

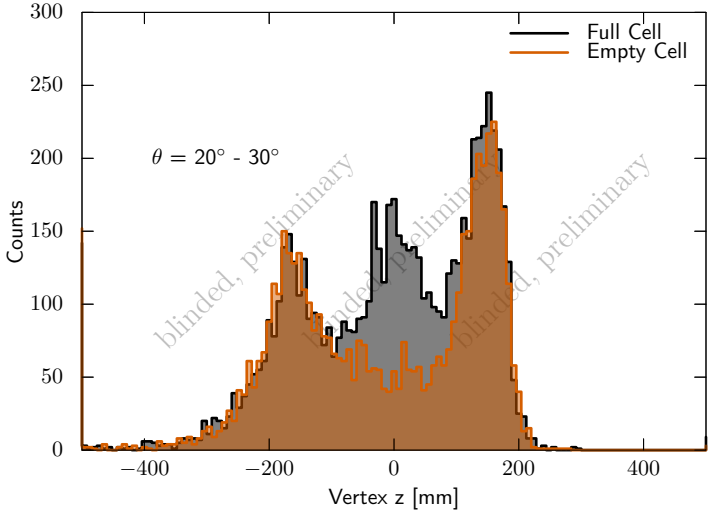

Note the width of the distribution here comes reflects multiple scattering of the beam in the full length of the LH_2 target.

LH2 Scattering

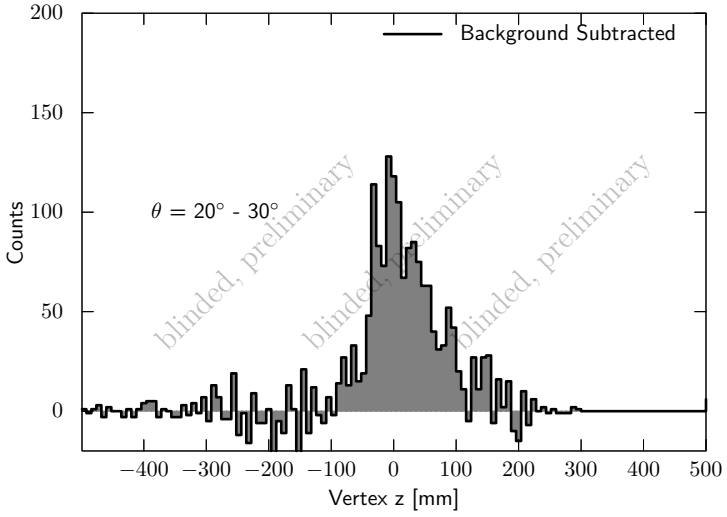

Note that background upstream of target consistent with 0.

LH2 Scattering

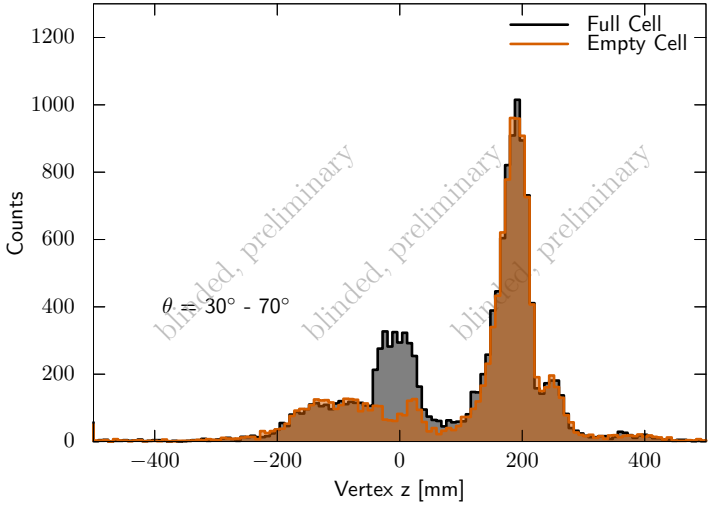

LH2 Scattering

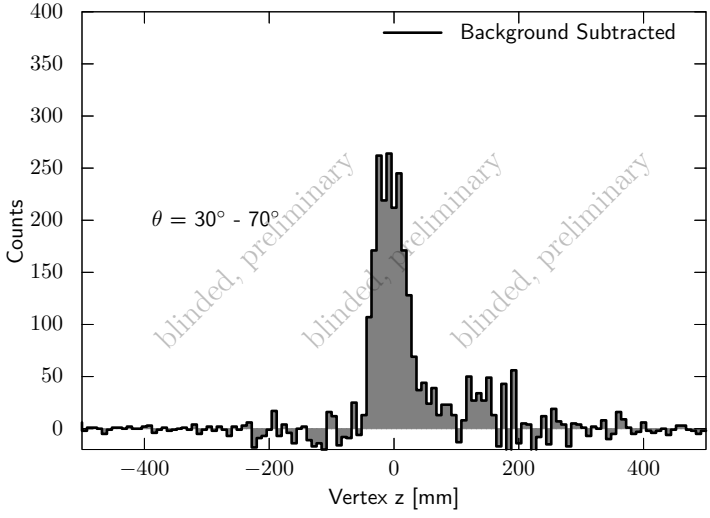

LH2 Scattering

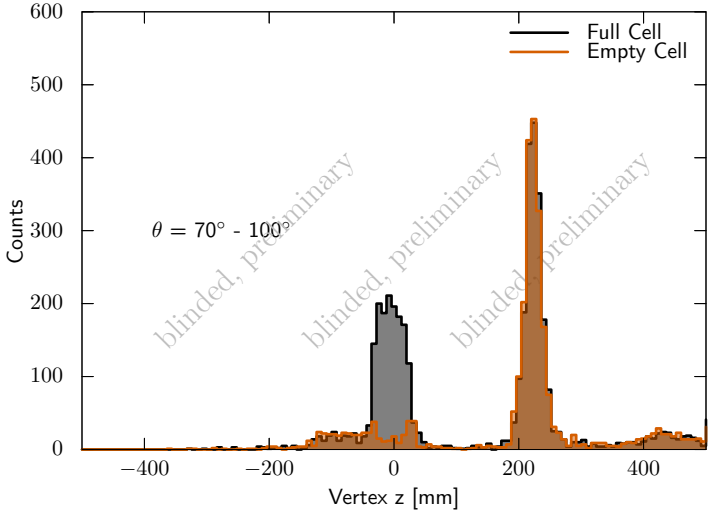

LH2 Scattering

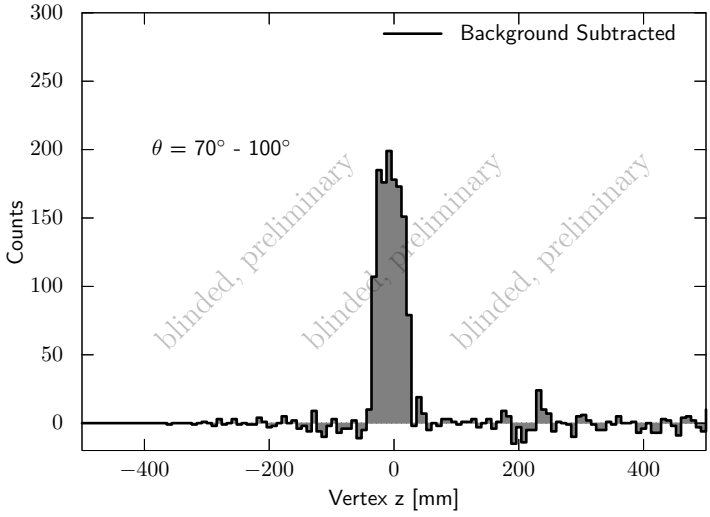

LH2 Scattering

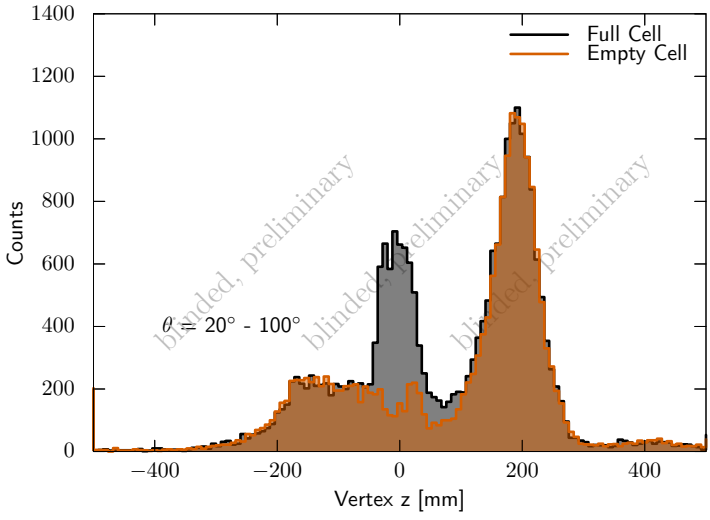

LH2 Scattering

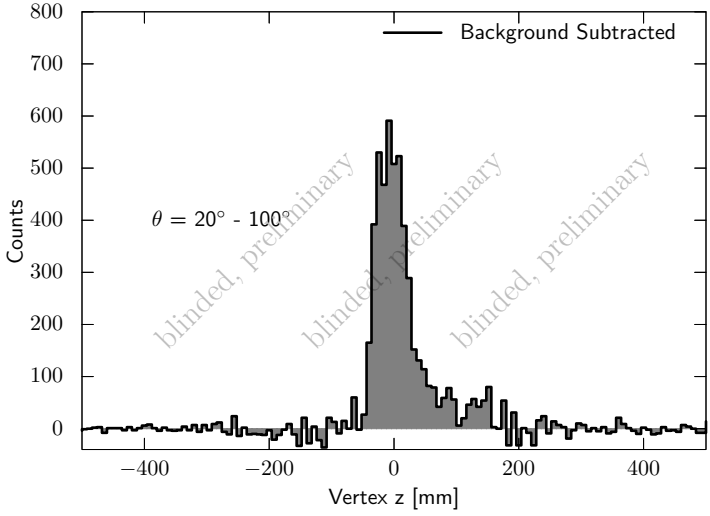

LH2 Scattering

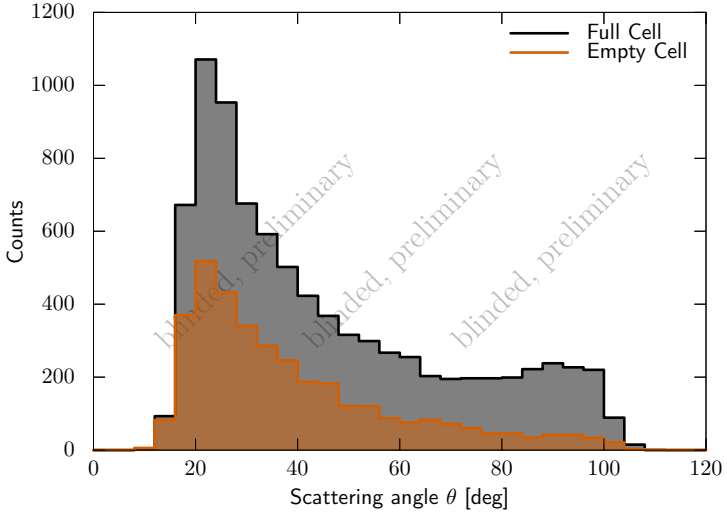

Here we present the reconstructed scattering angle from the full and empty cell. The blinding contribution is the same for both data sets, but in the empty cell there is primarily carbon scattering from the cell walls, which falls faster than the LH_2 cross section.

LH2 Scattering

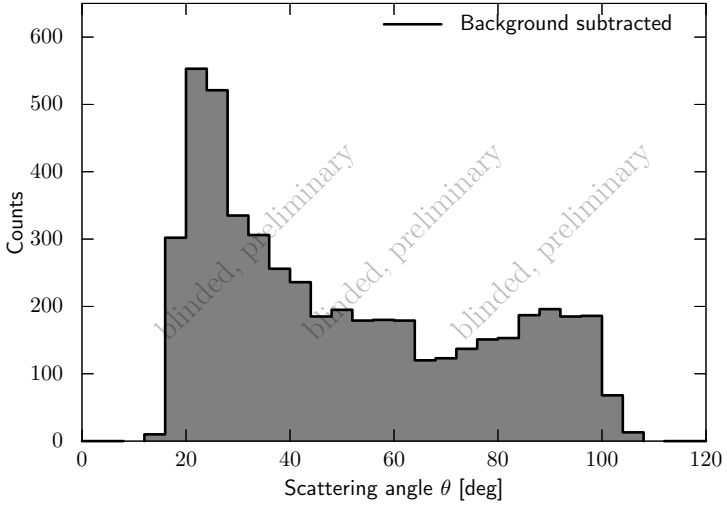

Background subtracted reconstructed scattering angle. Note blinding is implemented which can account for for the apparent excess events at backwards angles.

Expected Systematic Uncertainties on Cross Section

Uncertainty	angular distribution (%)	μ/e (%)	$+/-$ (%)
Detector efficiencies	0.1	0.1	0.1
Solid angle	0.1	small	small
Scattering angle offset	0.2	small	small
Multiple scattering	0.15	small	small
Beam momentum offset	0.1	0.1	0.1
Radiative correction	0.1 (μ), 0.5 (e)	0.5	1γ small
Magnetic contribution	0.15	small	small
Subtraction of μ decay	0.1	0.1	small
Target Subtraction	0.3	small	small
Beam PID	0.1	0.1	0.1
TOTAL	0.5 (μ), 0.7 (e)	0.5	0.2

from MUSE TDR https://arxiv.org/pdf/1709.09753.pdf.
Systematic uncertainties dominate statistical uncertainties for e and forward angle μ.

Measured Systematic Uncertainties on Cross Section

Uncertainty	angular distribution (%)	Measured (%)
Detector efficiencies	0.1	**0.1, cf. previous low level analysis talks** ✓
Solid angle	0.1	0.1, Requires full MC implementation *
Scattering angle offset	0.2	0.2, Survey implementation *
Multiple scattering	0.15	0.25, Vertex reconstruction cf. next slide *
Beam momentum offset	0.1	**0.05 cf. beam properties paper** ✓
Radiative correction	0.1 (μ), 0.5(e)	**0.1 (μ), 0.3 (e) cf. SS studies** ✓
Magnetic contribution	0.15	0.15 magnetic contribution in MUSE Q^2 ✓
Subtraction of μ decay	0.1	**0.1 Requires full statistics ***
Target Subtraction	0.3	0.3 Requires full statistics *
Beam PID	0.1	**0.1 from RF studies after vertexing ***
TOTAL	0.5 (μ), 0.7 (e)	0.52(μ), 0.59(e)

* Have yet to confirm in detail, but clear plan to study and affirm before radius results published.

✓On track to meet or exceed TDR estimates for uncertainty on radius.

Bold indicates uncertainties that do not cancel in cross section ratios, see previous slide.

Angular Resolution

- *If* poorer vertex resolution suggests worse angle resolution then systematic uncertainties increased
- **Worst case scenario:** acts like multiple scattering systematic, increases this systematic from 0.15 % to 0.25 %
- Arises from $\approx$ 25 mr contribution to angle determination
- Results will improve with full survey implementation

Summary

- Have reconstructed tracks from $e^- C$,$e^+ C$,and $e^+ H$ scattering
- In scattering off of hydrogen, background subtraction suppresses exit posts in data
  - Exact background subtraction requires MC
- See offsets in geometry between data and simulation
  - Vertex resolution worse in data than in simulation
- Blinded cross sections from $e^- C$,$e^+ C$ scattering extracted and compared to simulation and theory